

## Supporting Information

# Enhanced ammonia synthesis activity of carbon-supported Mo catalyst by Mo carburization

Biyun Fang, Chuanfeng Zhang, Jiahui Li, Miaodi Yang, Chunyan Li, Jun Ni, Xiuyun Wang,  
Jianxin Lin, Bingyu Lin\*, and Lilong Jiang\*

National Engineering Research Center of Chemical Fertilizer Catalyst, College of Chemical  
Engineering, Fuzhou University, Fuzhou, 350002 Fujian, China. E-mail: bylin@fzu.edu.cn (Bingyu  
Lin), jll@fzu.edu.cn (Lilong Jiang).

## 1. Experimental section

### 1.1. Preparation of Samples

**Preparation of thermally modified carbon.** Thermally modified carbon was prepared by the previous reported method.<sup>1</sup> Commercial activated carbon (AC, Fujian Xinsen Carbon. Co., Ltd.) was heated in Ar at 1900 °C for 2 h, and then oxidized in steam at 430 °C for 30 h. The resulting carbon was named as “C”, and the surface area of C was 713 m<sup>2</sup> g<sup>-1</sup>.

**Synthesis of MoO<sub>x</sub>/C.** Ammonium molybdate tetrahydrate ((NH<sub>4</sub>)<sub>6</sub>Mo<sub>7</sub>O<sub>24</sub>·4H<sub>2</sub>O) as Mo precursors, were introduced on C by incipient wetness impregnation, the weight ratio of Mo to C was 20 wt.%, and the sample was named as “the as-prepared MoO<sub>x</sub>/C”. The as-prepared sample was reduced in N<sub>2</sub>-H<sub>2</sub> at 500 °C for 6 h, and the reduced sample was named as MoO<sub>x</sub>/C.

**Synthesis of Mo<sub>2</sub>C/C catalysts.** The as-prepared MoO<sub>x</sub>/C was heated at 400 °C for 1 h with a heating rate of 10 °C min<sup>-1</sup> in H<sub>2</sub>. Subsequently, the sample continues to be heated from 400 to 700 °C at a rate of 1 °C min<sup>-1</sup> and held for 4 h. The sample drop to room temperature and then switch the gas to 0.5 %O<sub>2</sub>/Ar and keep it for 10 h to passivate the sample, and the resulting sample was named as “the as-prepared Mo<sub>2</sub>C/C”. The as-prepared sample was reduced in N<sub>2</sub>-H<sub>2</sub> at 500 °C for 6 h, and the reduced sample was named as Mo<sub>2</sub>C/C.

### 1.2. Characterization

X-ray diffraction (XRD) patterns were obtained in a PANalytical X'Pert3 Powder diffractometer

instrument with Cu K $\alpha$  radiation ( $\lambda=0.154\ 32\ \text{nm}$ ). Nitrogen absorption-desorption isotherms were measured at  $-196\ ^\circ\text{C}$  on ASAP 2020M instrument. Raman spectra were obtained using 532 nm laser by InVia Reflex Raman microscope equipped.

For Thermogravimetric analysis (TGA), 10 mg sample was heated to  $500\ ^\circ\text{C}$  under the 3.3 %  $\text{N}_2$ -10 %  $\text{H}_2$ -Ar gas mixture for 2 h and record the sample quality information by Setsys Evolution (Setaram) thermal analyzer.

The XPS results of the catalysts were collected using ESCALAB 250 X-ray photoelectron spectrometer. Before the measurements, the samples were reduced at  $500\ ^\circ\text{C}$  for 1h in a flow of 3.3 %  $\text{N}_2$ -10 %  $\text{H}_2$ -Ar mixture ( $30\ \text{ml}\ \text{min}^{-1}$ ) in the pretreatment chamber. After cooling down to  $50\ ^\circ\text{C}$ , the sample was transferred into the analysis chamber during which the samples do not contact air. Binding energy calibration was performed using adventitious carbon ( $284.6\ \text{eV}$ ) before data processing.

The D/H exchange experiment was carried out on Micromeritics AutoChem II 2920 equipment. First, 100 mg sample was raised to  $500\ ^\circ\text{C}$  at  $10\ ^\circ\text{C}\ \text{min}^{-1}$  in hydrogen atmosphere and maintained for 2 h and then purged with Ar for 30 min and cooled down to  $400\ ^\circ\text{C}$ . After that, the gas was changed to  $\text{D}_2$  and keep sample at  $400\ ^\circ\text{C}$  for 60 min. After reduce the temperature to  $50\ ^\circ\text{C}$  in  $\text{D}_2$  and continue to maintain it for 60 min, the mass signals were recorded by a Hiden Analytical HPR-20 spectrometer while changing the gas to 3.3 %  $\text{N}_2$ -10 %  $\text{H}_2$ -Ar gas mixture. Temperature-programmed surface reaction (TPSR) was performed after the D/H exchange. The sample temperature was heated to  $600\ ^\circ\text{C}$  at  $10\ ^\circ\text{C}\ \text{min}^{-1}$  and record the mass spectrometry signal.

Temperature-programmed desorption of hydrogen or nitrogen ( $\text{H}_2$ -TPD or  $\text{N}_2$ -TPD) experiments was carried out on the same instrument. After reduced in  $\text{H}_2$  at  $500\ ^\circ\text{C}$  for 6 h, catalyst was purged and cooled to  $400\ ^\circ\text{C}$  in Ar. Afterwards, hydrogen or nitrogen was added to sample for 1 h and cooled to  $50\ ^\circ\text{C}$ . Finally, the sample was heated in Ar flow to  $600\ ^\circ\text{C}$ , and the TCD signals were obtained.

### **1.3. Evaluation of catalytic performance**

Catalytic reactions were conducted in a continuous fixed-bed flow (inner diameter = 12 mm). The catalyst was reduced by temperature programmed reduction program  $500\ ^\circ\text{C}$  in  $\text{N}_2$ - $\text{H}_2$  (1:3) atmosphere for 6 h, then ammonia synthesis activity test was carried out under the set conditions (each condition was stable for at least 2 h). Afterward the outlet gas of the reactor was absorbed by

fixed volume of dilute sulfuric acid aqueous solution. The ammonia synthesis rate was calculated based on the concentration of ammonium ion in the solution by ion chromatography. The reproducibility of the reaction rate was confirmed 3 times and the error range was  $\pm 5\%$ .

#### 1.4. Reaction order

To measure the reaction orders with respect to  $N_2$  and  $H_2$ , 0.2 g of catalyst was loaded into the reactor and the gas flow rate was fixed at  $120 \text{ mL min}^{-1}$ . The ammonia synthesis tests are carried out under the conditions without mass transport or heat transfer limitations, and the detailed mass transport and heat transfer calculations based on the best-performing  $Mo_2C/C$  have been given above. The ammonia concentration in the outlet gas is lower than 5% under the adopted condition, and thus the change in the ammonia partial pressure would exert a negligible influence on the measured partial pressures of nitrogen and hydrogen. In view of this, the influence of the ammonia partial pressure on the reaction orders of  $N_2$  and  $H_2$  is slight. The constituent gases of the reactant ( $N_2$ ,  $H_2$ , Ar) were as follows in volume fraction (10%, 50%, 40%), (20%, 50%, 30%) and (34%, 50%, 16%) for  $N_2$  order, (20%, 30%, 50%), (20%, 50%, 30%) and (20%, 80%, 0) for  $H_2$  order. The  $NH_3$  order was obtained by changing the flow rate of a stoichiometric  $H_2-N_2$  gas mixture ( $60-240 \text{ mL min}^{-1}$ ). The kinetic experiments were carried out far from equilibrium conditions, and the reaction orders were calculated according to the methods described elsewhere.<sup>2</sup> The reaction orders were estimated by using the following Eqs:

$$r = kP_{N_2}^\alpha P_{H_2}^\beta P_{NH_3}^\gamma \quad (1)$$

$$r = \frac{1}{W} \frac{dy_0}{d\left(\frac{1}{q_0}\right)} \quad (2)$$

$$my_0^{m-1} dy_0 = Cd\left(\frac{1}{q_0}\right) \quad (3)$$

$$C = k_2 P_{N_2}^\alpha P_{H_2}^\beta \quad (4)$$

Where  $r$  is the ammonia synthesis rate,  $\alpha$ ,  $\beta$ , and  $\gamma$  are the reaction orders with respect to  $N_2$ ,  $H_2$ , and  $NH_3$ , respectively.  $P_{N_2}$ ,  $P_{H_2}$ , and  $P_{NH_3}$  are the partial pressures of  $N_2$ ,  $H_2$ , and  $NH_3$ , respectively. And  $W$ ,  $y_0$  and  $q_0$  represent the catalyst mass, molar fraction of ammonia in the outlet gas and relationship between flow rate.

#### 1.5 Mass and Heat Transfer Calculations for Ammonia Synthesis over $Mo_2C/C$

Mears Criterion for External Diffusion (Fogler, Elements of Chemical Reaction Engineering, 4th edition, p841; Mears, Ind. Eng. Chem. Process Des. Dev. 1971, 10, 541–547)

$$\text{If } C_M = \frac{(-r'_A)\rho_b R n}{k_c C_{Ab}} < 0.15, \text{ then external mass transfer effects can be neglected.}$$

$-r'_A$  = reaction rate of nitrogen, kmol/kg-cat·s

n = reaction order with respect to N<sub>2</sub>.

R = catalyst particle radius, m

$\rho_b$  = bulk density of catalyst bed, kg/m<sup>3</sup>

$C_{Ab}$  = bulk gas concentration of nitrogen, kmol/m<sup>3</sup>

$k_c$  = mass transfer coefficient, m/s

$$C_M = \frac{(-r'_A)\rho_b R n}{k_c C_{Ab}} = [2.7 \times 10^{-7} \text{ kmol-N}_2/\text{kg-cat}\cdot\text{s}][910 \text{ kg/m}^3][3 \times 10^{-4} \text{ m}][0.69]/([1.7 \text{ m/s}][0.045 \text{ kmol/m}^3]) = 6.7 \times 10^{-7} < 0.15$$

Generally, according to the Mears Criterion, when the calculation value for  $C_M$  is below 0.15, the external diffusion limitations can be neglected during the kinetic experiments. In our case, the  $C_M$  is  $6.7 \times 10^{-7}$ , indicating that the external diffusion limitations of the kinetic experiments could be neglected.

Weisz-Prater Criterion for Internal Diffusion (Fogler, Elements of Chemical Reaction Engineering, 4th edition, p839)

$$\text{If } C_{WP} = \frac{(-r'_A)\rho_c R^2}{D_e C_{As}} < 1, \text{ then internal mass transfer effects can be neglected.}$$

$-r'_A$  = reaction rate of nitrogen, kmol/(kg-cat·s)

$\rho_c$  = solid catalyst density (kg m<sup>-3</sup>)

R = catalyst particle radius, m

$\rho_c$  = bulk density of catalyst bed, kg/m<sup>3</sup>

$C_{Ab}$  = bulk gas concentration of nitrogen, kmol/m<sup>3</sup>

$k_c$  = mass transfer coefficient, m/s

$D_e$  = effective gas-phase diffusivity (m<sup>2</sup> s<sup>-1</sup>)

$$C_{WP} = \frac{(-r'_A)\rho_c R^2}{D_e C_{As}} = [2.7 \times 10^{-7} \text{ kmol-N}_2/\text{kg-cat}\cdot\text{s}] \times [4 \times 10^3 \text{ kg-cat/m}^3] \times [3 \times 10^{-4} \text{ m}]^2 / ([3.34 \times 10^{-6} \text{ m}^2/\text{s}] \times [0.045 \text{ kmol/m}^3]) = \mathbf{6.5 \times 10^{-4} < 1}$$

Generally, according to the Mears Criterion, when the calculation value for  $C_{WP}$  is below 1, the internal diffusion limitations can be neglected during the kinetic experiments. In our case, the  $C_{WP}$  is  $6.5 \times 10^{-4} < 1$ , indicating that the internal diffusion limitations of the kinetic experiments could be neglected.

Mears Criterion for External (Interphase) Heat Transfer (Fogler, Elements of Chemical Reaction Engineering, 4th edition, p842)

$$C_{MH} = \left| \frac{-\Delta H_r (-r'_A) \rho_b R E}{h_t T_b^2 R_g} \right| < 0.15$$

$$[136.9 \text{ kJ/mol} \times 2.7 \times 10^{-7} \text{ kmol-N}_2/\text{kg-cat}\cdot\text{s} \times 910 \text{ kg-cat/m}^3 \times 3 \times 10^{-4} \text{ m} \times 150 \text{ kJ/mol}] / [185.3 \text{ kJ/m}^2\cdot\text{K}\cdot\text{s} \times 673^2 \text{ K}^2 \times 8.314 \times 10^{-3} \text{ kJ/mol}\cdot\text{K}] = \mathbf{2.2 \times 10^{-10} < 0.15}$$

Generally, according to the Mears Criterion, when the calculation value for  $C_{MH}$  is below 0.15, the heat transfer effect can be neglected during the kinetic experiments. In our case, the  $C_{MH}$  is  $2.2 \times 10^{-9}$ , indicating that the heat transfer effect can be neglected in the kinetic experiments.

Mears Criterion for Combined Interphase and Intraparticle Heat and Mass Transport (Mears, Ind.

Eng. Chem. Process Des. Dev. 1971, 10, 541–547)

$$\frac{(-r_A')\rho_b R^2}{D_e C_{Ab}} < \frac{1 + 0.33\gamma\chi}{|n - r_b\beta_b|(1 + 0.33n\omega)}$$

$$\gamma = \frac{E}{R_g T_s}; \quad \gamma_b = \frac{E}{R_g T_b}; \quad \beta_b = \frac{(-\Delta H_r) D_e C_{Ab}}{\lambda T_b}; \quad \chi = \frac{(-\Delta H_r)(-r_A')R}{h_t T_b}; \quad \omega = \frac{(-r_A')R}{k_c C_{Ab}}$$

$\gamma$  = Arrhenius number;

$\beta_b$  = heat generation function;

$\lambda$  = catalyst thermal conductivity, W/m.K;

$\chi$  = Damköhler number for interphase heat transport

$\omega$  = Damköhler number for interphase mass transport

$$\frac{(-r_A')\rho_b R^2}{D_e C_{Ab}} = [2.7 \times 10^{-7} \text{ kmol-N}_2/\text{kg-cat}\cdot\text{s} \times 910 \text{ kg-cat/m}^3 \times (3 \times 10^{-4})^2 \text{ m}^2] / ([3.34 \times 10^{-6} \text{ m}^2/\text{s}] \times [0.045 \text{ kmol/m}^3]) = \mathbf{1.5 \times 10^{-4}}$$

$$\frac{1 + 0.33\gamma\chi}{|n - r_b\beta_b|(1 + 0.33n\omega)} = \mathbf{1.1}$$

Left member < Right member

Generally, according to the Mears Criterion, when the calculation value for  $\frac{(-r_A')\rho_b R^2}{D_e C_{Ab}}$  is lower

than that for  $\frac{1 + 0.33\gamma\chi}{|n - r_b\beta_b|(1 + 0.33n\omega)}$ , the interphase and intraparticle heat and mass transfer effect can be neglected during the kinetic experiments.

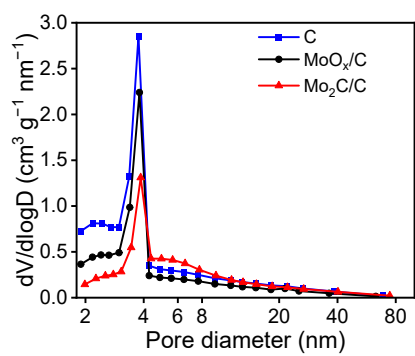


Fig. S1 Pore size distribution map of C,  $\text{MoO}_x/\text{C}$  and  $\text{Mo}_2\text{C}/\text{C}$ .

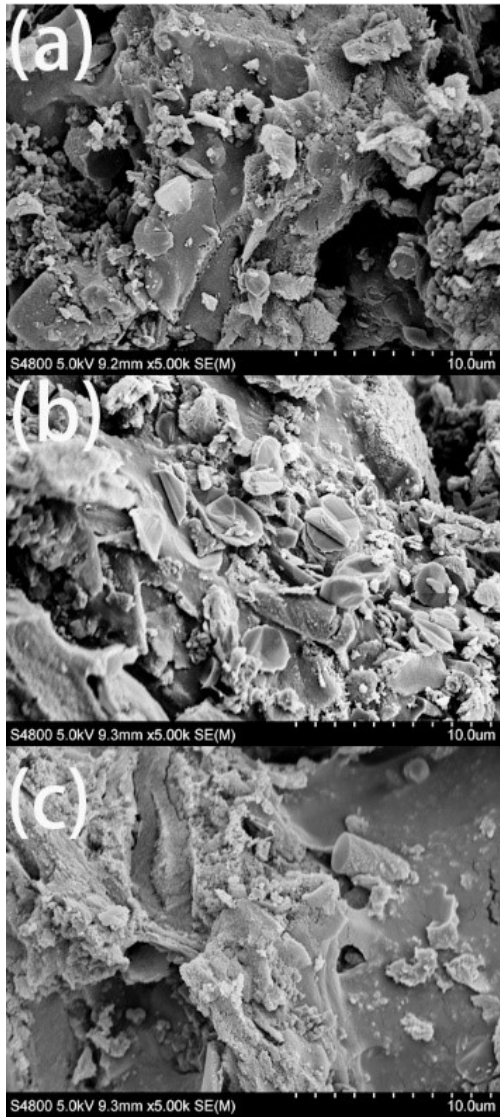
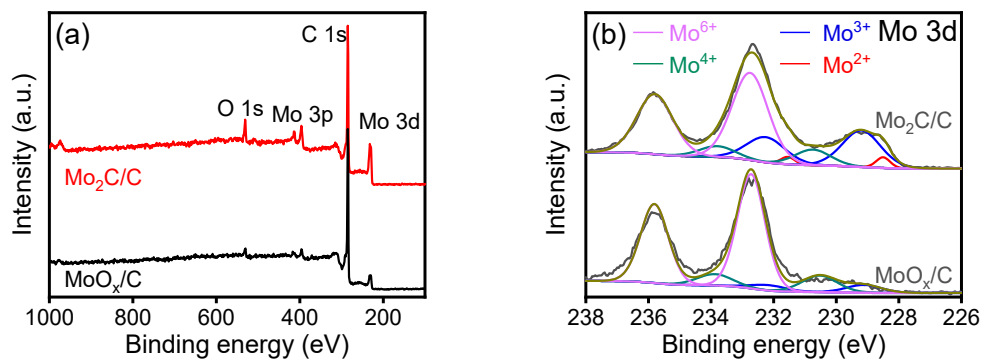


Fig. S2 SEM images of (a) C, (b) MoO<sub>x</sub>/C, (c) Mo<sub>2</sub>C/C.



Fi

g. S3 (a) XPS survey spectra and (b) Mo 3d XPS spectra of the as-prepared Mo catalysts without hydrogen treatment.

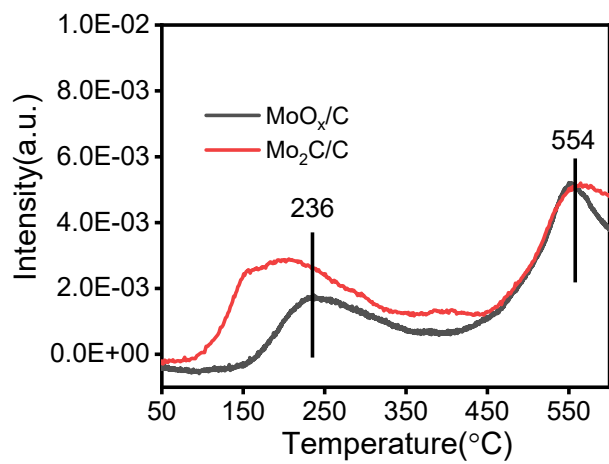


Fig. S4 N<sub>2</sub>-TPD profiles of Mo catalysts.

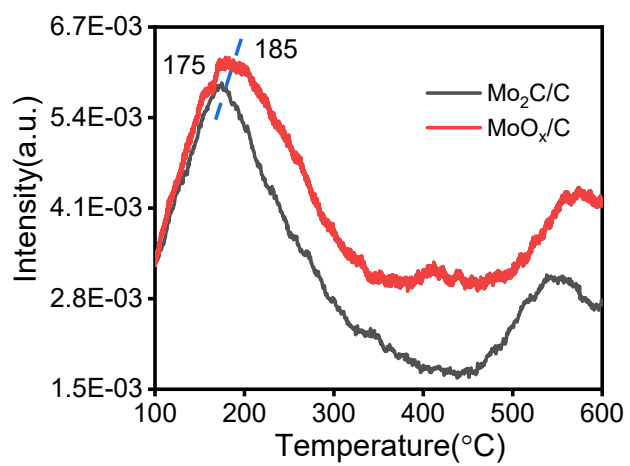


Fig. S5 H<sub>2</sub>-TPD profiles of Mo catalysts.

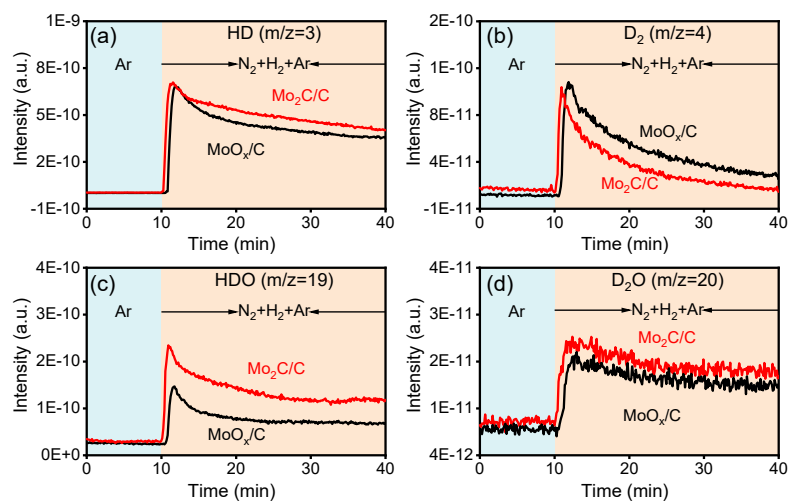


Fig. S6 The mass signals of HD, D<sub>2</sub>, HDO, and D<sub>2</sub>O with time during the D/H exchange reaction at 50 °C.

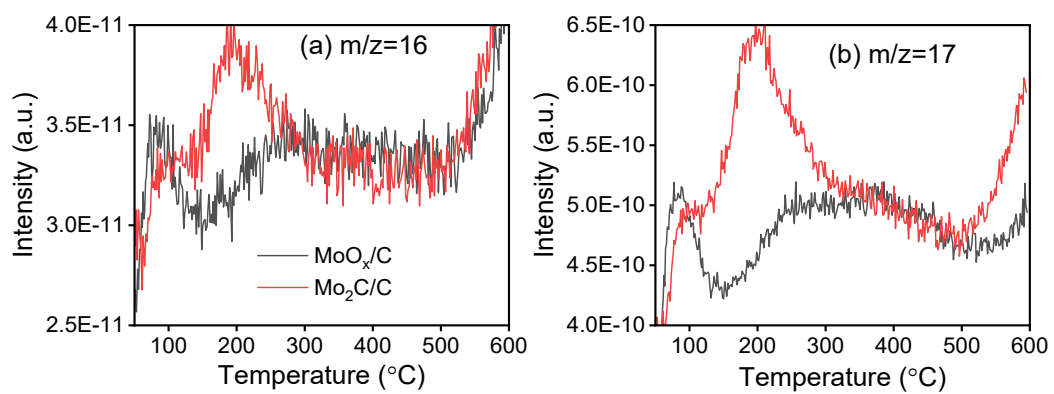


Fig. S7 Evolution profiles of  $\text{NH}_2$  ( $m/z=16$ ) and  $\text{NH}_3$  ( $m/z=17$ ) during TPSR study in the 3.3%  $\text{N}_2$ -10%  $\text{H}_2$ -Ar mixture.

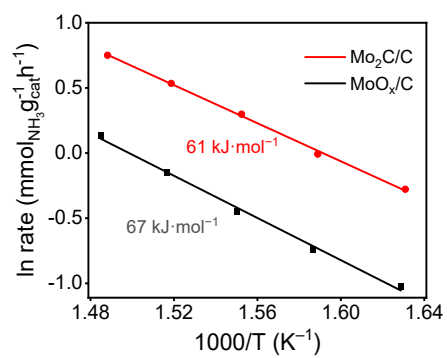


Fig. S8 Arrhenius plots of ammonia synthesis for MoO<sub>x</sub>/C and Mo<sub>2</sub>C/C.

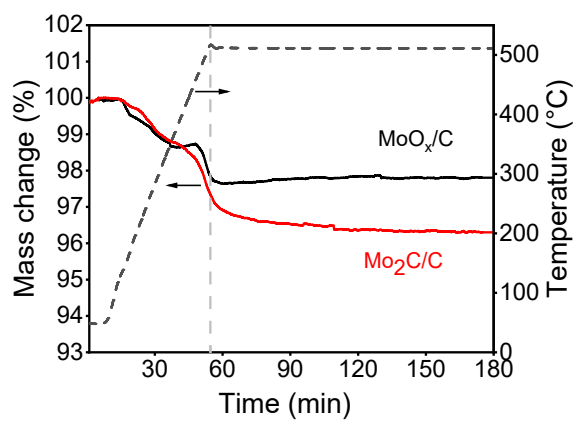


Fig. S9 TG profiles of Mo catalyst in 3.3 %N<sub>2</sub>-10 %H<sub>2</sub>-Ar gas mixture.

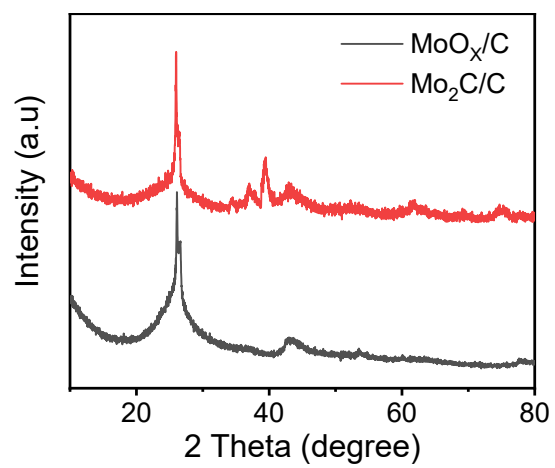


Fig. S10 XRD patterns of used catalysts.

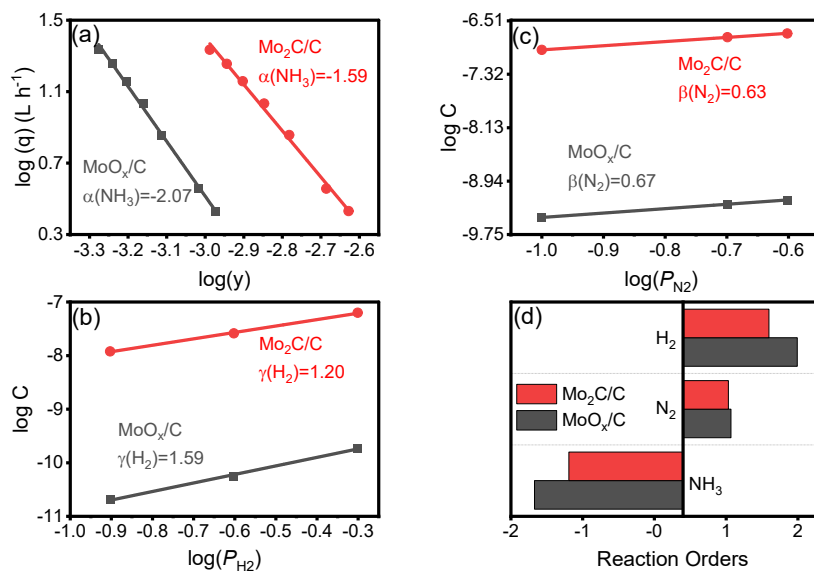


Fig. S11 Graphs for calculating reaction orders with respect to (a)  $\text{NH}_3$ , (b)  $\text{H}_2$ , (c)  $\text{N}_2$  and (d)  $\text{H}_2$ ,  $\text{N}_2$  and  $\text{NH}_3$  reaction orders, and the reproducibility of the reaction rate is confirmed 3 times and the error range is  $\pm 5\%$ .

Table S1 Textural properties of MoO<sub>x</sub>C/C and Mo<sub>2</sub>C/C catalysts.

Sample	Surface area (m <sup>2</sup> g <sup>-1</sup> )	Pore Volume (cm <sup>3</sup> g <sup>-1</sup> )	Average pore diameter (nm)	I <sub>D</sub> /I <sub>G</sub>
C	713	0.64	3.7	1.45
MoO <sub>x</sub> /C	424	0.41	3.9	1.22
Mo <sub>2</sub> C/C	272	0.36	5.2	0.85

Table S2 CO chemisorption results and particle sizes obtained by TEM measurements.

Samples	CO quantity <sup>a</sup> ( $\mu\text{mol/g}_{\text{cat}}$ )	Dispersion <sup>a</sup> (%)	Particle size <sup>b</sup> (nm)
MoO <sub>x</sub> /C	11.6	0.66	8.1
Mo <sub>2</sub> C/C	22.8	1.28	10.1

<sup>a</sup> obtained by CO chemisorption;

<sup>b</sup> obtained by TEM measurement (more than 100 particles).

Table S3 Ammonia synthesis activities of Mo catalysts.

Samples	Rate (mmol g <sub>cat</sub> <sup>-1</sup> h <sup>-1</sup> )	Ea (kJ mol <sup>-1</sup> )	Reaction conditions	SV (mL g <sup>-1</sup> h <sup>-1</sup> )	Ref.
MoO <sub>x</sub> /C	1.05	67	1 MPa, 400 °C	36 000	This
Mo <sub>2</sub> C/C	1.95	61	1 MPa, 400 °C	36 000	Work
γ-Mo <sub>2</sub> N	0.29	51	1 MPa, 400 °C	9 000	3
β-Mo <sub>2</sub> C	1.70	53	1 MPa, 400 °C	9 000	4
Co <sub>3</sub> Mo <sub>3</sub> N	1.07	57	1 MPa, 400 °C	9 000	
Co-Mo/CeO <sub>2</sub>	2.84	--	0.9 MPa, 400 °C	72 000	5
Mo/Co-CeO <sub>2</sub>	2.72	57	1 MPa, 400 °C	72 000	6
Mo/Co-CeO <sub>2</sub>	1.29	57	1 MPa, 400 °C	36 000	6
CoMo/CeO <sub>2</sub>	0.48	61	1 MPa, 400 °C	36 000	6

Table S4 The Mo loading of Mo catalysts obtained by ICP analysis and N content obtained by Elemental Analysis.

Samples	Mo loading (wt%)	N content (wt%)
MoO <sub>x</sub> /C	16.5	< 0.3
Mo <sub>2</sub> C/C	15.6	< 0.3
Used MoO <sub>x</sub> /C	16.8	< 0.3
Used Mo <sub>2</sub> C/C	15.2	< 0.3

References:

1. B. Lin, K. Wei, X. Ma, J. Lin and J. Ni, *Catalysis Science & Technology*, 2013, **3**, 1367–1374.
2. (a) R. Kojima and K.-i. Aika, *Applied Catalysis A: General*, 2001, **218**, 121–128; (b) Y. Tsuji, K. Ogasawara, M. Kitano, K. Kishida, H. Abe, Y. Niwa, T. Yokoyama, M. Hara and H. Hosono, *J. Catal.*, 2018, **364**, 31-39.
3. R. Kojima and K.-i. Aika, *Applied Catalysis A: General*, 2001, **219**, 141-147.
4. R. Kojima and K.-i. Aika, *Applied Catalysis A: General*, 2001, **218**, 121–128.
5. Y. Tsuji, M. Kitano, K. Kishida, M. Sasase, T. Yokoyama, M. Hara and H. Hosono, *Chem Commun (Camb)*, 2016, **52**, 14369–14372.
6. B. Fang, Z. Qi, F. Liu, C. Zhang, C. Li, J. Ni, J. Lin, B. Lin and L. Jiang, *J. Catal.*, 2022, **406**, 231–240.